Molecules and Cells

Characterization of αX I-Domain Binding to Receptors for Advanced Glycation End Products (RAGE)

Dolgorsuren Buyannemekh, and Sang-Uk Nham*

Divisions of Science Education and Biology, Kangwon National University, Chuncheon, Chuncheon 24341, Korea
*Correspondence: sunham@kangwon.ac.kr
http://dx.doi.org/10.14348/molcells.2017.0021
www.molcells.org

The β2 integrins are cell surface transmembrane proteins regulating leukocyte functions, such as adhesion and migration. Two members of β2 integrin, αMβ2 and αXβ2, share the leukocyte distribution profile and integrin αXβ2 is involved in antigen presentation in dendritic cells and transendothelial migration of monocytes and macrophages to atherosclerotic lesions. Receptor for advanced glycation end products (RAGE), a member of cell adhesion molecules, plays an important role in chronic inflammation and atherosclerosis. Although RAGE and αXβ2 play an important role in inflammatory response and the pathogenesis of atherosclerosis, the nature of their interaction and structure involved in the binding remain poorly defined. In this study, using I-domain as a ligand binding motif of αXβ2, we characterize the binding nature and the interacting moieties of αX I-domain and RAGE. Their binding requires divalent cations (Mg^{2+} and Mn^{2+}) and shows an affinity on the sub-micro molar level: the dissociation constant of αX I-domains binding to RAGE being 0.49 μM. Furthermore, the αX I-domains recognize the V-domain, but not the C1 and C2-domains of RAGE. The acidic amino acid substitutions on the ligand binding site of αX I-domain significantly reduce the I-domain binding activity to soluble RAGE and the alanine substitutions of basic amino acids on the flat surface of the V-domain prevent the V-domain binding to αX I-domain. In conclusion, the main mechanism of αX I-domain binding to RAGE is a charge interaction, in which the acidic moieties of αX I-domains, including E244, and D249, recognize the basic residues on the RAGE V-domain encompassing K39, K43, K44, R104, and K107.

Keywords: β2 integrin, binding, I-domain, leukocytes, RAGE

INTRODUCTION

The β2 integrins are cell surface transmembrane proteins regulating leukocyte functions, such as adhesion, spreading, migration, and phagocytosis (Hynes, 2002; Tan, 2012). These proteins consist of a common β2 subunit and four specific α subunits: αL, αM, αX, and αD (Arnaout, 2002). The binding of β2 integrins to their ligands is mostly mediated through a distinct motif of the α subunits, namely, the I-domain, which contains a metal ion dependent adhesion site (MIDAS) (Lee et al., 1995). The α subunits of β2 integrin (αM and αX) are closely related, with 63% sequence identity and the αMβ2 and αXβ2 integrins bind to a largely overlapping array of ligands, including iC3b, fibrinogen, heparin, and ICAM-1 (Luo et al., 2007; Stacker and Springer, 1991). The αMβ2 and αXβ2 integrins share a leukocyte distribution profile, both being present on circulating neutrophils, monocytes, and macrophages. Whereas αMβ2 is the dominant β2 integrin on neutrophils, αXβ2 is the major β2 integrin on dendritic cells and tissue-resident macrophages (Hogg et al., 1986). αMβ2 plays an important role in neutrophil transmigration, while αXβ2 is involved in the antigen presentation in dendritic cells and transendothelial migration of monocytes

Received 10 February, 2017; revised 13 April, 2017; accepted 27 April, 2017; published online 24 May, 2017

eISSN: 0219-1032
© The Korean Society for Molecular and Cellular Biology. All rights reserved.
This is an open-access article distributed under the terms of the Creative Commons Attribution-NonCommercial-ShareAlike 3.0 Unported License. To view a copy of this license, visit http://creativecommons.org/licenses/by-nc-sa/3.0/.

and macrophages to atherosclerotic lesions (Meunier et al., 1994; Wu et al., 2009).

Receptor for advanced glycation end products (RAGE) is a member of the immunoglobulin (Ig) protein family of cell surface molecules and consists of three extracellular Ig domains (namely, V, C1, and C2) linked with a single transmembrane helix and a cytoplasmic domain (Sims et al., 2010). RAGE was first identified as an advanced glycation end products (AGEs) receptor, but was later found to be a member of the cell adhesion molecule (CAM) family. It was reported that RAGE binds to various ligands encompassing high mobility group box-1(HMGB-1 or amphoterin), amyloid β peptide, transthyretin, and members of the S100 (Deane et al., 2003; Hofmann et al., 1999; Hori et al., 1995; Sousa et al., 2000). After engagement of these molecules, RAGE starts a series of signaling events, eventually leading to chronic inflammation, atherosclerosis, and diabetes. RAGE is also involved in leukocyte adhesion and migration after binding to β2 integrins. It was shown that RAGE is expressed at a high level on inflamed endothelial or intestinal epithelial cells that promote transmigration of leukocytes (Frommhold et al., 2010; Zen et al., 2007). Furthermore, RAGE was found to bind purified αXβ2 and αMβ2 *via* the I-domain (Chavakis et al., 2003).

Although RAGE and αXβ2 play an important role in inflammatory response and the pathogenesis of atherosclerosis, the nature of their interaction and structure involved in the binding remain less defined. Therefore, in this study, we attempted to characterize the binding nature and important moieties of the molecules mediating their interaction. We now report that the main mechanism of αX I-domain binding to RAGE is a charge interaction with a moderate binding affinity and that the acidic moieties of αX I-domains are involved in the recognition of the basic residues on the V-domain of RAGE.

MARERIALS AND METHODS

Production of Glutathione S-transferase (GST) fusion proteins

The *E.coli* strain BL21 was the host strain for all pGEX vector derived plasmids expressing GST-αM I, GST-αX I, and GST-αX I-domain mutants. The expression and purification of GST-αX I-domain and GST-αX I-domain mutants have been previously described elsewhere (Choi et al., 2010). GST-αM I-domain was expressed by *E. coli* host bearing an expression plasmid pEXCD11b, which was constructed by the insertion of a cDNA fragment encoding human αM I-domain (a.a. 112-318) at the Bam HI site of pGEX4T1 (GE Healthcare, USA).

Production of recombinant RAGE proteins

Recombinant RAGE fused with the human IgG Fc region produced from mammalian cells was purchased from R&D Systems (USA). This protein, containing the ecto domain of RAGE, was immobilized on a CM5 chip for the surface plasmon resonance (SPR) analysis.

For other fragments of RAGE, a full length ecto domain (V, C1, and C2), V-domain, and C-domain (C1 and C2) of RAGE were expressed and purified from *Pichia pastoris* as His-tagged proteins. A fragment of cDNA encoding a full length RAGE ecto domain (a.a. 26-341) was ligated into a *Pichia* expression vector, pPICαA (Invitrogen, USA) for the soluble RAGE expression. For the soluble RAGE V and C-domain production, cDNAs encoding the V-domain (a.a. 26-122) and C-domain (a.a. 124-341) were inserted into pPICαA. The resultant expression plasmids were introduced into *Pichia pastoris* cells *via* electroporation at 1.5 kV, 25 μF, and 200 ohms. The induction and purification of sRAGE and sRAGE domains were performed according to a previous report (Higgins, 1995).

For bacterial expression of alanine substituted mutants of the RAGE V-domain, cDNA encoding RAGE V-domain was subjected to site-directed mutagenesis as previously described (Choi et al. 2005). Then, the cDNAs encoding the RAGE V-domain mutants were inserted into a bacterial expression vector, pET21a (EMD Millipore, USA), and introduced into *E.coli* strain BL21 (DE3). All expression vectors contained an ancillary nucleotide sequence encoding 43 amino acids, including hexa-histidine tag, and were verified by DNA sequencing. The induction and purification of the RAGE V-domain and its mutants were performed according to the previously reported manual (Sambrook and Russell, 2001).

Enzyme-linked immunosorbent assay (ELISA)-based binding assay

Ligand proteins at the concentration of 10.0 μg/ml in PBS (10 mM phosphate buffer, 150 mM NaCl, pH 7.4) were added to each well in microtiter plates (Immulon, USA) and incubated overnight at 4℃. The plates were washed with PBS and blocked for 2 h with a blocking buffer (PBS with 5% bovine serum albumin). The microtiter plates were then loaded with analyte proteins (usually 100 μl) in a binding medium (50 mM Tris/HCl, pH 7.4, 150 mM NaCl, 5% bovine serum albumin, 1 mM $MgCl_2$) and incubated for 1 hour. The plates were washed with PBS and 0.1% Triton X100 and further incubated for 1 hour with anti-GST antibody (1/2000 dilution, BD Pharmingen, USA) or Ni-NTA conjugated with alkaline phosphatase (1/2000 dilution, HisDetector Nickel-AP, KPL, USA) to detect the GST fusion protein or His-tagged protein, respectively. Following the washing step, anti-mouse IgG conjugated with alkaline phosphatase was loaded and incubated for 1 hour. Alkaline phosphatase substrate, Bluephos™ (KPL, USA), was loaded after washing. The color intensity of each well was measured by absorbance readings at 595 nm (Biorad microplate reader 550, USA).

Characterization of binding by the surface plasmon resonance (SPR) analysis

The SPR experiments were performed on a Biacore X (GE Healthcare). Recombinant RAGE fused with human IgG Fc or GST-αX I-domain was covalently immobilized on the respective carboxy-methyl dextran chip (CM5) *via* primary amino groups, according to the manufacturer's instructions. For each chip, an activated and blocked flow channel was used as a reference to correct for bulk effects and nonspecific

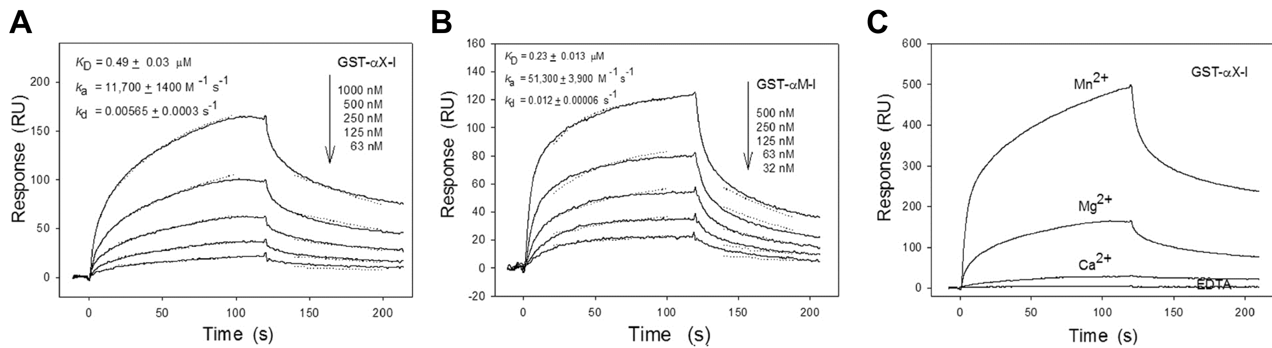

Fig. 1. Kinetic analysis of αX and αM I-domain binding to RAGE and the effect of cations on these bindings. SPR sensogram of GST-αX-I (A) and GST-αM-I (B) binding to the immobilized RAGE-Fc on a CM5 chip at 3000 RU. The responses (solid line) from the injection of various concentrations of the I-domain are overlaid with the fit of a 1:1 interaction model (dotted line) in the region of kinetic analysis for association and dissociation rate constants. The dissociation constant (K_D) of I-domain was calculated by three independent SPR experiments of RAGE and αX and αM I-domain binding. (C) αX I-domain (1 μM) was injected to flow over immobilized RAGE-Fc, in the presence of divalent cations (1 mM) or EDTA (3 mM).

binding. The analytes were diluted in a running buffer (150 mM NaCl, 10 mM HEPES, pH 7.4, 1 mM 1 mM $MgCl_2$). Bound proteins were removed with a regeneration buffer (300 mM NaCl, 20 mM EDTA, 20 mM Tris/HCl, pH 8.0). For the kinetic analysis, the analytes were injected for 120 s for association; thereafter, dissociation data were collected for 120 s, all at the speed of 30 μl/min. For the simple binding test, the analytes were injected for 90 s for association; then, dissociation data were collected for 90 s, all at the speed of 20 μl/min. Binding curves were obtained by subtracting bulk change and nonspecific binding. Binding kinetics were analyzed by BIAevaluation 3.0 software. Dissociation constant (K_D), association rate constant (k_a), and dissociation rate constant (k_d) were calculated by curve fitting of association and dissociation phases by using the 1:1 Langmuir binding model.

RESULTS

To characterize the nature of αXβ2 binding to RAGE, the binding kinetics of the interaction should be determined. In this study, we employed αX I-domain for measuring the binding affinity as a ligand binding motif of αXβ2 and αM I-domain for comparing the binding properties of αX I-domain to RAGE. The dissociation constant (K_D) and other kinetic values were measured from the three independent SPR experiments and subsequent analysis. As shown in one of the SPR sensorgrams (Figs.1A and 2B), all binding curves (solid lines) generally fitted well to the 1:1 Langmuir binding model (dotted lines), showing a good fit in the region of kinetic analysis for association and dissociation rate constants. From the kinetic analysis, the dissociation constants of αX and αM I-domain binding to RAGE were calculated to be 0.49 and 0.23 μM, respectively. This result indicates that the affinity of αX I-domain is a sub-micro molar level and is lower than that of αM I-domain approximately a half of that for αM I-domain. The lower binding affinity of αX I-domain is attributed by approximately one fourth of the αM I-domain association rate constant (k_a) value and a half of the αM I-domain dissociation rate constant (k_d) value. This suggests that αX I-domain associates RAGE four times slower than αM I-domain and dissociates from RAGE two times slower than αM I-domain. The kinetics data of αM I-domain binding we observe are largely consistent with the results of a previous study where the dissociation constant of purified αMβ2 to soluble RAGE was assessed to be approximately 0.2 μM in an ELISA-based binding assay (Chavakis et al., 2003).

The binding of αX I-domain to RAGE was specific and required divalent cations, such as Mn^{2+} and Mg^{2+}, but not Ca^{2+} (Fig. 1C). In addition, the effect of Mn^{2+} ion for RAGE binding in αX I-domain is higher than Mg^{2+}. These results are also consistent with the data of many other integrin I-domains that bind divalent cations for ligand recognition.

RAGE consists of three immunoglobulin-like domains (V, C1, and C2) and cytoplasmic tails linked to the transmembrane region (Sims et al., 2010). In order to establish the binding domain of RAGE for β2 integrin, the soluble RAGE, V, and C type domains were expressed with His-tag sequences and purified from *Pichia Pastoris* to homogeneity (Figs. 2A and 2B). Soluble RAGE and other domains were injected to flow over I-domain immobilized CM5 chips for comparison of their binding patterns to I-domains. As shown in the SPR sensorgram (Fig. 2C), sRAGE and sRAGEV bind well with immobilized αX I-domain, whereas sRAGEC1/2 does not, suggesting that the V domain of RAGE is responsible for αXβ2 integrin binding. This finding is also supported by the results of the ELISA-based binding analysis: immobilized αX I-domain associates with sRAGEV well, but not with sRAGEC1/2 (Fig. 2D) and immobilized sRAGE and sRAGEV bind well to the αX and αM I-domains but not to GST (Figs. 2E and 2F). In line with our previous kinetic data, the binding levels of αM I-domain to sRAGE and sRAGEV are higher than those to αX I-domain.

To further understand the binding nature of RAGE and αX I-domains, we tested sRAGE and sRAGEV binding to αX I-domain mutants (K242A/K243A, E244A, D249M, K251A,

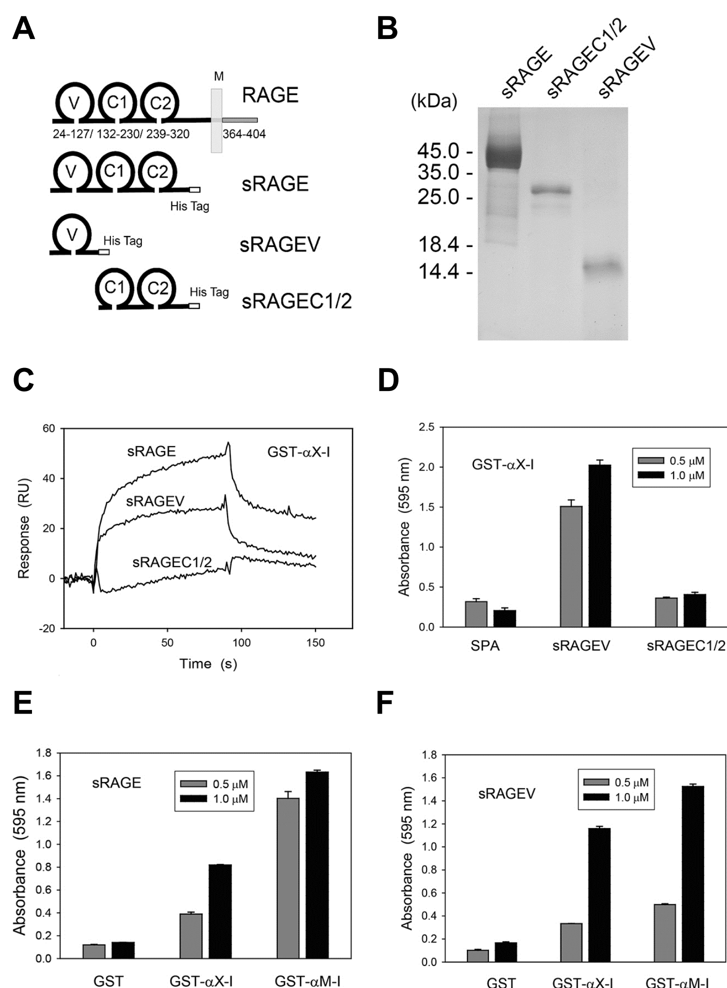

Fig. 2. Binding of αX and αM I-domains to RAGE and the V-domain of RAGE. (A) A schematic representation of recombinant RAGE and RAGE derived soluble domains. All soluble proteins are fused with a His-tag for purification and detection. (B) SDS-PAGE analysis of purified sRAGE, sRAGEC1/2 and sRAGEV. (C) SPR sensorgram of sRAGE and RAGE-derived soluble domains binding to immobilized GST-αX-I. RAGE-derived proteins (1 μM) were injected to flow over immobilized GST-αX-I on a CM5 sensor chip (1800 RU). (D) Binding of sRAGEV and sRAGEC1/2 to GST-αX-I on microtiter plates. sRAGEV and sRAGEC1/2 (0.5 μM or 1.0 μM) were loaded on microtiter plates coated with GST-αX-I. Data are means ± S. E. (n = 3). (E, F) Binding of the I-domains to the sRAGE (E) and sRAGEV (F) on microtiter plates. GST and αX and αM I-domains (0.5 μM or 1.0 μM) were loaded on microtiter plates coated with sRAGE and sRAGEV. Data are means ± S. E. (n = 3).

and E298S/D299T) which are alanine or non-charged amino acid substitutions of selected basic, or acidic amino acid residues near a groove traversing ligand binding surface (Fig. 3A). In earlier studies, these mutant I-domains proved to be useful in terms of identifying the nature of the interaction of I-domain and its ligands (Choi et al., 2005; Lee et al., 2007). In Figs. 3B and 3C, the substitutions of negatively charged amino acids (E244A, D259M, and E298S/D299T) lower the binding strengths of αX I-domain to sRAGE and sRAGEV. By contrast, alanine substitutions of positively charged residues (K242A/K243A and K251A) raise the αX I-domain binding activity. These results suggest a charge interaction between RAGE and αX I-domain, in which the acidic residues of αX I-domain surface are responsible for recognizing amino acid residues on the V-domain of RAGE.

To further investigate the role of acidic residues of αX I-domain, selected mutants of the I-domain (K242A/K243A, E244A, and D249M) were subjected to the SPR experiments for the binding kinetic analysis. As shown in Table 1, the measured dissociation constants (K_D) of αX I-domain mutants (E244A and D249M) for RAGE are higher than that of wild type, whereas K_D of K242A/K243A is lower, indicating the critical importance of acidic residues of I-domain in the recognition of RAGE. Notably, the high K_D values of E244A and D249M are mainly attributed by approximately a half of the wild type αX I-domain association rate constant (k_a) value, suggesting that these mutant I-domains bind to RAGE slower than in the case of the binding of wild type I-domain. On the other hand, K242A/K243A shows the same level of k_a value as wild type αX I-domain, but approximately 2/3 of the wild type αX I-domain dissociation rate constant (k_d) value, suggesting that K242A/K243A dissociates slower from RAGE than wild type. These results provide convincing evidence on the critical importance of acidic residues of αX I-domain for the recognition of RAGE in the mechanism of electrostatic interaction during the association phase, as well as a secondary role of basic residues to modulate the interaction during the dissociation phase.

Unlike other domains of RAGE, the V-domain of RAGE is highly basic. An electropotential surface map of RAGE domain (Fig. 4A) shows a front flat face and an opposite convex face, as well as a positively charged region which runs across a front face and wraps around the opposite face of the domain. Several positive residues of this positive region were shown to play a critical role to recognize RAGE ligands, such as AGEs and S100B (Koch et al., 2010; Matsumoto et

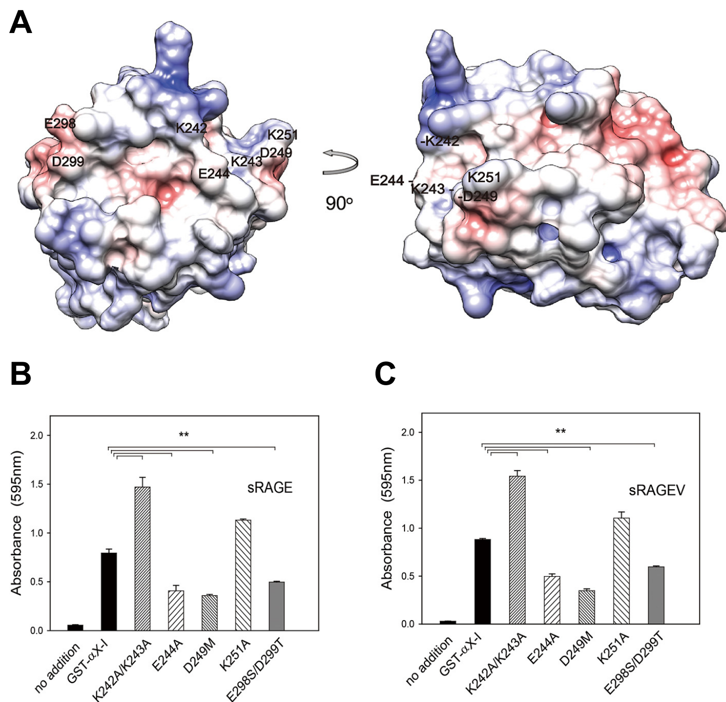

Fig. 3. Binding of αX I-domain mutants to sRAGE or sRAGEV. (A) A crystal structure of the αX I-domain showing molecular surface and the side chain of amino acid residues subjected to mutagenesis. A molecular surface representation of the αX I-domain was based on the crystal structure, PDB # 1N3Y (Vorup-Jensen et al., 2003). The surface electropotential map of αX I-domain was drawn by an UCSF Chimera computer program (Pettersen et al., 2004) with Adaptive Poisson-Boltzman Solver software package (Baker et al., 2001) and expressed as two color patterns: blue represents positively charged area, and red represents negatively charged region. (B, C) Binding of αX I-domain mutants to the sRAGE (B) and sRAGEV (C). In the mutant name, the first letter indicates the amino acid residue at the position of αX amino acid sequence, and the second letter at the right hand side of the number shows the changed amino acid. αX I-domain mutants (1 μM) were incubated in microtiter plate wells pre-coated with sRAGE and sRAGEV. Data are mean ± S. E (n = 3). $**P < 0.01$ (Student t-test).

Table 1. Binding kinetics of αX I-domain mutants to RAGE

Analyte	dissociation constant K_D (10^{-6} M)	association rate constant k_a ($M^{-1}S^{-1}$)	dissociation rate constant k_d (S^{-1})
GST-αX-I	0.49 ± 0.03	11,700 ± 1400	0.0056 ± 0.0003
K242A/K243A	0.37 ± 0.03	12,100 ± 790	0.0040 ± 0.0005
E244A	0.97 ± 0.10	4,790 ± 900	0.0045 ± 0.0005
D249M	1.08 ± 0.05	6,120 ± 420	0.0060 ± 0.0009

RAGE-Fc was immobilized on a CM5 chip (3000 RU).
All data are shown as means ± S. E. (N = 3).

al., 2008). To delineate the critical residues for I-domain binding, we performed alanine substitutions of several positively charged amino acids in the positive region of the V-domain (K37, K39, K43, K44, and R104), as well as K107 that locates at the edge of the basic area. These mutants and wild type V-domains were expressed as N terminus His-tag fusion form in *E.coli* and purified to homogeneity for testing their binding activities.

As shown in Fig. 4B, the alanine substitutions of all positive residues substantially reduce the binding activity of the V-domain to αX I-domain. All mutations, except for K37A, also decrease the binding strength of RAGE to αM I-domain (Fig. 4C). These results indicate that positively charged residues, including K39, K43, K44, R104, and K107, are involved in the recognition of the αM and αX I-domain. Taken together, these results allow us to conclude that there is a charge interaction as a mechanism of RAGE and αX I-domain binding.

DISCUSSION

Our results demonstrate that αX I-domain binds to RAGE with an affinity on the sub-micro molar level (K_D = 0.49 μM) in a divalent cation-dependent manner. Furthermore, αX I-domain recognizes the V-domain, but not the C1 and C2-domains of RAGE. The main mechanism of αX I-domain binding to RAGE is a charge interaction, in which the acidic moieties of αX I-domains, including E244 and D249, recognize the basic residues on the RAGE V-domain encompassing K39, K43, K44, R104, and K107.

A molecular surface representation of the αX I-domain shows a unique feature of the αX I-domain: there is a groove traversing ligand binding surface at the “top” of the domain (Fig. 3A). This groove is surrounded by the acidic residues E244, D249, E298, and D299, and is interrupted by basic residues K242 and K243. Although there is a high level of homology between αM and αX I-domains, αM I-domain possesses more acidic residues than αX I-domain in a groove spanning ligand binding surface. There are two substitutions of acidic residues in αM (E244 and E253) for basic residues in αX (K242 and K251) near the groove. Moreover, the groove on αM I-domain is not interrupted by positively charged amino acids, such as K242 and K243, as in the case of αX I-domain. In addition, K245 in αM, which is equivalent to K243 of αX, is buried inside of the molecule to form hydrogen bonds to other residues of surrounding α helixes nearby the groove. These molecular characteristics may contribute αM I-domain to have a higher affinity for RAGE than αX I-domain.

The alanine substitutions of several positive residues reduced the binding activity of the V-domain to both αM and

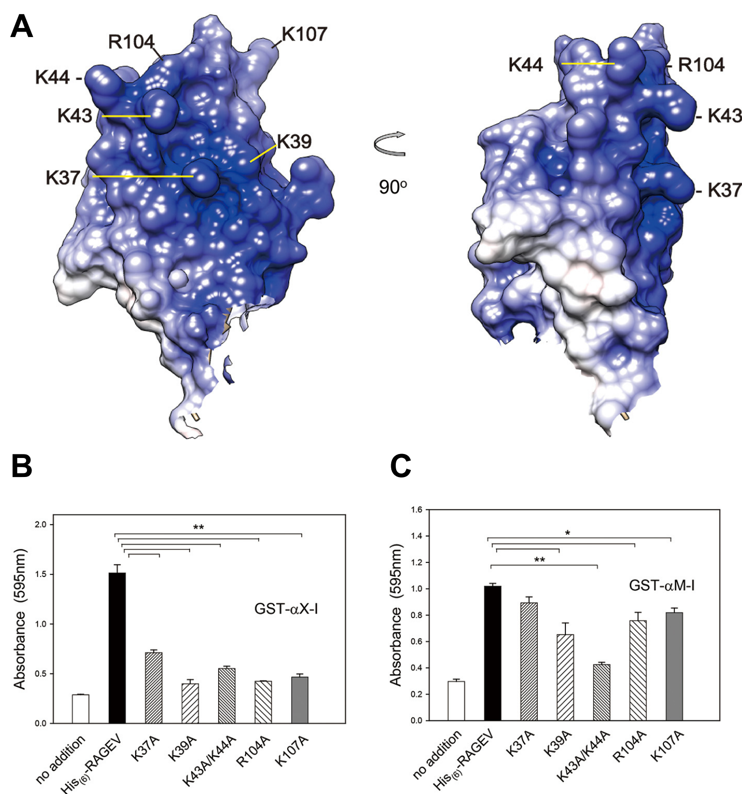

Fig. 4. Binding of RAGE V-domain and its mutants to αX and αM I-domains. (A) A molecular surface representation of the RAGE V-domain, PDB # 3CJJ (Sturchler et al., 2008) drawn by an UCSF Chimera computer program, with the electrostatic potential mapped on the surface. As shown in Fig. 3, blue and red represents positively and negatively charged areas, respectively. (B, C) Binding of RAGE V-domain and V-domain mutants to GST-αX-I (B) and GST-αM-I (C) on microtiter plate wells. These proteins were incubated at a concentration of 1 μM. Data are mean ± S. E (n = 3). *$P < 0.05$, **$P < 0.01$ (Student *t*-test).

αX I-domains (Figs. 4B and 4C). Notably, the mutations of the V-domain (K37A, K39A, K43A/K44A, R104A, and K107A) have less effect on αM I-domain binding than on αX I-domain. This difference can be explained by the different molecular characteristics of the I-domains: αM I-domain has more acidic residues on its ligand binding surface and a higher affinity for the V-domain than αX I-domain. When a particular positive amino acid is replaced by alanine in the V-domain, one charge interaction previously formed by the positive residue gets lost between αM I-domain and the alanine substituted V-domain. But other charge interactions between the two molecules still remain, therefore, αM I-domain binding to the V-domain is not substantially decreased. Contrary to this, αX I-domain binding to the mutant V-domain is significantly reduced. Because αX I-domain has less acidic moieties on its ligand binding surface than αM I-domain, the sum of remaining charge interactions of αX I-domain with the V-domain is weaker than that of αM I-domain. The different surface charges and affinities for the V-domain might be the reason for the different effects of the alanine substitutions of the V-domain on the binding of the I-domains.

In previous research, integrin αXβ2 was shown to recognize the acidic residues of decayed proteins by denaturation or cleaved proteins by proteolytic enzymes (Vorup-Jensen et al., 2005). It was reported that αX I-domain binds the acidic residues of ligands, such as fragment E, Thy-1, plasminogen, and ICAM-1, by employing the positively charged amino acids (K242 and K243) on the ligand binding surface of the I-domain (Choi et al., 2005; 2010; Gang et al., 2007; Lee et al,2007). However, the mechanism of αX I-domain binding to RAGE appears to be different from the other ligands. Whereas the acidic residues of αX I-domain play a critical role by forming salt bridges with complementary ionic pairs in the V-domain of RAGE, the basic residues of αX I-domain are involved in a secondary and modulatory role. Although there is a limited area on a metal ion-dependent adhesion site (MIDAS), αX I-domain can bind various and unrelated ligands. This multivalency of αXβ2 for several ligands can be partially explained by this mechanism, the different usage of charged amino acids on the ligand binding surface of the MIDAS.

While all three domains of RAGE can serve as binding sites for various ligands, most of ligands recognize the V-domain of RAGE (Kierdorf and Fritz, 2013). As exceptional cases, S100A6 interacts with C1 and C2 RAGE domains and amyloid-β aggregates bind to the C1-domain (Leclerc et al., 2007; Sturchler et al., 2008). The present study revealed that, as most of RAGE ligands, β2 integrin, αMβ2 and αXβ2, also interact with the V-domain of RAGE.

There are many positively charged amino acids on the surface of the V-domain of RAGE (Fig. 4A). Among these amino acids, residues K43, K44, R48, K52, R98, and R104 play a critical role to bind BSA conjugated AGE, and residue R48, R98, and R104 for S100B recognition (Koch et al., 2010; Matsumoto et al., 2008). Our results demonstrate several basic residues (K39, K43, K44, R104, and R107) in the V-domain of RAGE as crucial amino acids for αMβ2 and αXβ2.

It should be noted that these amino acid sequences, but not K37, are evolutionary conserved in mammals from mouse to human, indicating the significant role of the charged amino acids on the function of RAGE. This result also suggests that αMβ2 and αXβ2 may share the same binding site of the V-domain with AGEs and S100B in an overlapping, but not identical manner.

Although the binding mechanism of β2 integrin to RAGE is generally similar to other RAGE ligands, one feature is quite different: whereas most RAGE ligands have a tendency to form oligomers, β2 integrin does not. The AGE modification of proteins causes a multiple covalent cross-links, leading to higher molecular mass molecules. Furthermore, S100B and several S100A proteins to form larger assembles, ranging from tetramers to octamers (Korndorfer et al., 2007; Zieman and Kass, 2004). The oligomerization of these RAGE ligands appears to increase of binding strengths for RAGE, resulting in an enhancement of signals which lead to inflammation and atherosclerosis. As cell surface proteins which cannot form oligomers, β2 integrins have different mechanisms to modulate their binding abilities for RAGE.

There are two mechanisms for regulating the strength of integrin binding to their ligands: (1) affinity modulation by a conformational change of integrin and (2) avidity modulation by varying the degree of integrin clustering (Luo et al., 2007). The I-domains used in this study are activated forms by a small truncation from the α7 helix of the I-domains, being considered to have a high affinity conformation (Xiong et al., 2000). The data in this report indicate that the binding affinity of αX I-domain for RAGE (0.49 μM) is lower than that of αM I-domain (0.23 μM). Considering that the expression level of αXβ2 on leukocytes is not as high as αMβ2, it is conceivable that αXβ2 does not make a considerable contribution to leukocyte adhesion and transmigration.

However, several reports have provided some evidence demonstrating the significance of αXβ2 interaction with RAGE during monocyte adhesion, especially at the early onset of atherosclerosis. A critical step in the initial stage of atherosclerosis is the recruitment of inflammatory monocytes and their differentiation into foamy macrophages in nascent plaque. By using $CD11c^{-/-}$ mice (αXβ2 deficient mice), Wu et al. showed that αXβ2 expression is elevated on blood monocytes during hypercholesterolemia and αXβ2 is involved in the formation of atherosclerotic lesions (Wu et al., 2009). Furthermore, Foster et al. revealed that a high level of lipoproteins in the blood causes both affinity and avidity up-regulation of αXβ2 in a subset of monocytes, resulting in a firm monocyte adhesion onto inflamed endothelium (Foster et al., 2015).

In this study, the binding affinity of αX I-domain for RAGE (0.49 μM) appears to be higher than those for other αXβ2 ligands expressed on activated endothelial cell surface such as Thy-1 (1.16 μM) and ICAM-1 (0.73 μM) as shown in previous reports (Choi et al., 2005; 2010). This relative high affinity of αXβ2 for RAGE further emphasizes the significance of interaction between αXβ2 and RAGE. Therefore, further analysis of the interaction between αXβ2 and RAGE may provide useful insights for future biomedical studies aiming to develop potential therapeutics for atherosclerosis.

ACKNOWLEDGMENTS

We are grateful for the technical support provided by the Central Laboratory of Kangwon National University. This study was supported by 2013 Research Grant from Kangwon National University (No. 120131270).

REFERENCES

Arnaout, M.A. (2002). Integrin structure: new twists and turns in dynamic cell adhesion, Immunol. Rev. *186,* 125-140.

Baker, N.A., Sept, D., Joseph, S., Holst, M.J., and McCammon, J.A. (2001). Electrostatics of nanosystems: application to microtubules and the ribosome. Proc. Natl. Acad. Sci. USA *98*, 10037-10041.

Chavakis, T., Bierhaus, A., Al-Fakhri, N., Schneider, D., Witte, S., Linn, T., Nagashima, M., Morser, J., Arnold, B., Preissner, K.T., et al. (2003). The pattern recognition receptor (RAGE) is a counterreceptor for leukocyte integrins: a novel pathway for inflammatory cell recruitment. J. Exp. Med. *198*, 1507-1515.

Choi, J., Leyton, L., and Nham, S.-U. (2005). Characterization of αX I-domain binding to Thy-1. Biochem. Biophy. Res. Comm. *331*, 557-561.

Choi, J., Choi, J., and Nham, S.-U. (2010). Characterization of the residues of αX I-domain and ICAM-1 mediating their interactions. Mol. Cells *30*, 227-234.

Deane, R., Yan, S.D., Submamaryan, R.K., LaRue, B., Jovanovic, S., Hogg, E., Welch, D., Manness, L., Lin, C., Yu, J., et al. (2003). RAGE mediates amyloid-beta peptide transport across the blood-brain barrier and accumulation in brain. Nat. Med. *9*, 907-913.

Foster, G.A., Xu, L., Chidambaram, A.A., Soderberg, S.R., Armstrong, E.J., Wu, H., and Simon, S.I. (2015). CD11c/CD18 signals Very Late Antigen-4 activation to initiate foamy monocyte recruitment during the onset of hypercholesterolemia. J. Immunol. *195*, 5380-5392.

Frommhold, D., Kamphues,A., Hepper, I., Pruenster, M., Lukic, I.K., Socher, I., Zablotskaya, V., Buschmann, K., Lange-Sperandio, B., Schymeinsky, J., et al. (2010). RAGE and ICAM-1 cooperate in mediating leukocyte recruitment during acute inflammation *in vivo*. Blood *116*, 841-849.

Gang, J., Choi, J., Lee, J.H., and Nham, S.-U. (2007). Identification of critical residues for plasminogen binding by the αX I-domain of the β2 integrin, αXβ2, Mol. Cells *24*, 240-246.

Higgins, D.R. (1995). Heterologous protein expression in the methylotrophic yeast Pichia pastoris, in: J.E. Coligan, B.M. Dunn, H.L. Ploegh, D.W. Speicher, P.T. Wingfield., eds., (Current protocols in protein science, John Wiley & Sons, Inc.), pp. 5.7.1-5.7.16.

Hofmann, M.A., Drury, S., Fu, C., Qu, W., Taguchi, A., Lu, Y., Avila, C., Kambham, N., Bierhaus, A., Nawroth, P., et al. (1999). RAGE mediates a novel proinflammatory axis: a central cell surface receptor for S100/calgranulin polypeptides. Cell *97*, 889-901.

Hogg, N., Takacs, L., Palmer, D.G., Selvendran, Y., and Allen, C. (1986). The p150,95 molecule is a marker of human mononuclear phagocytes: comparison with expression of class II molecules. Eur. J. Immunol. *16*, 240-248.

Hori, O., Brett, J., Slattery, T., Cao, R., Zhang, J., Chen, J.X., Nagashima, M., Lundh, E.R., Vijay, S., Nitecki, D., et al. (1995). The receptor for advanced glycation end products (RAGE) is a cellular binding site for amphoterin. J. Biol. Chem. *270*, 25752-25761.

Hynes, R.O. (2002). Integrins: bidirectional, allosteric signaling machines. Cell *110*, 673-687.

Kierdorf, K., and Fritz, G. (2013). RAGE regulation and signaling in inflammation and beyond. J. Leukoc. Biol. *94*, 55-68.

Koch, M., Chitayat, S., Dattilo, B.M., Schiefner, A., Diez, J., Chazin, W.J., and Fritz, G. (2010). Structural basis for ligand recognition and activation of RAGE. Structure *18*, 1342-1352.

Korndorfer, I. P., Brueckner, F., and Skerra, A. (2007). The crystal structure of the human (S100A8/S100A9)2 heterotetramer, calprotectin, illustrates how conformational changes of interacting alpha-helices can determine specific association of two EF-hand proteins. J. Mol. Biol. *370*, 887-898.

Leclerc, E., Fritz, G., Weibel, M., Heizmann, C.W., and Galichet, A. (2007). S100B and S100A6 differentially modulate cell survival by interacting with distinct RAGE (receptor for advanced glycation end products) immunoglobulin domains. J. Biol. Chem. *282*, 31317-31331.

Lee, J.O., Rieu, P., Arnaout, M.A., and Liddington, R.C. (1995). Crystal structure of the A domain from the α subunit of integrin CR3 (CD11b/CD18). Cell *80*, 631-638.

Lee, J.H., Choi, J., and Nham, S.-U. (2007). Critical residues of αX I-domain recognizing fibrinogen central domain. Biochem. Biophys. Res. Comm. *355*, 1058-1063.

Luo, B.-H., Carman, C.V., and Springer, T.A. (2007). Structural basis of integrin regulation and signaling. Annu. Rev. Immunol. *25*, 619-647

Matsumoto, S., Yoshida,T., Murata, H., Harada, S., Fujita, N., Nakamura, S., Yamamoto, Y., Watanabe, T., Yonekura, H., Yamamoto, H., et al. (2008). Solution structure of the variable-type domain of the receptor for advanced glycation end products: new insight into AGE-RAGE interaction. Biochemistry *47*, 12299-12311.

Meunier, L., Bohjanen, K., Voorhees, J.J., and Cooper, K.D. (1994). Retinoic acid upregulates human Langerhans cell antigen presentation and surface expression of HLA-DR and CD11c, a β2 integrin critically involved in T-cell activation. J. Invest. Dermatol. *103*, 775-779.

Pettersen, E.F., Goddard, T.D., Huang, C.C., Couch, G.S., Greenblatt, D.M., Meng, E.C., and Ferrin, T.E. (2004). UCSF Chimera-a visualization system for exploratory research and analysis. J. Comput. Chem. *25*, 1605-1612.

Sambrook, J., and Russell, D.W. (2001). Purification of histidine-tagged proteins by immobilized Ni^{2+} absorption chromatography, in: Molecular Cloning, a laboratory manual, (Cold Spring Harbor Laboratory Press, New York), pp. 15.44-15.48.

Sims, G.P., Rowe, D.C., Rietdijk, S.T., Herbst, R., and Coyle, A.J. (2010). HMGB1 and RAGE in inflammation and cancer. Annu. Rev. Immunol. *28*, 367-388.

Sousa, M.M., Yan, S.D., Stern, D., and Saraiva, J.M. (2000). Interaction of the receptor for advanced glycation end products (RAGE) with transthyretin triggers nuclear transcription factor kB (NF-kB) activation. Lab. Invest. *80*, 1101-1110.

Stacker, S.A., and Springer, T.A. (1991). Leukocyte integrin P150,95 (CD11c/CD18) functions as an adhesion molecule binding to a counter-receptor on stimulated endothelium. J. Immunol. *146*, 648-655.

Sturchler, E., Galichet, A., Weibel, M., Leclerc, E., and Heizmann, C.W. (2008). Site-specific blockade of RAGE-Vd prevents amyloid-β oligomer neurotoxicity. J. Neurosci. *28*, 5149-5158.

Tan, S. M. (2012). The leucocyte β2 (CD18) integrins: the structure, functional regulation and signaling properties. Biosci. Rep. *32,* 241-269.

Vorup-Jensen, T., Ostermeier, C., Shimaoka, M., Hommel, U., and Springer, T.A. (2003). Structure and allosteric regulation of the αXβ2 integrin I-domain. Proc. Natl. Acad. Sci. USA *100*, 1873-1878.

Vorup-Jensen, T., Carman, C.V., Shimaoka, M., Schuck, P., Svitel, J., and Springer, T.A. (2005). Exposure of acidic residues as a danger signal for recognition of fibrinogen and other macromolecules by integrin αXβ2. Proc. Natl. Acad. Sci. U S A. *102*, 1614-1619.

Wu, H., Gower, R.M., Wang, H., Perrard, X.-Y., Ma, R., Bullard, D.C., Burns, A.R., Paul, A., Smith, C.W., Simon, S.I., et al. (2009). Functional role of $CD11c^{+}$ monocytes in atherogenesis associated with hypercholesterolemia. Circulation *119*, 2708-2717.

Xiong, J.P., Li, R., Essafi, M., Stehle, T., and Arnaout, M.A. (2000). An isoleucine-based allosteric switch controls affinity and shape shifting in integrin CD11b A-domain. J. Biol. Chem. *275*, 38762-38768.

Zen, K., Chen, C.X., Chen, Y.T., Wilton, R., and Liu, Y. (2007). Receptor for advanced glycation endproducts mediates neutrophil migration across intestinal epithelium. J. Immunol. *178*, 2483-2490.

Zieman, S.J., and Kass, D.A. (2004). Advanced glycation endproduct crosslinking in the cardiovascular system: potential therapeutic target for cardiovascular disease. Drugs *64*, 459-470.